

Muon charge ratio using the CORSIKA simulation code

M. Bahmanabadi^{1,2,*} and M. Fazlalizadeh^{3,†}

¹*Department of Physics, Sharif University of Technology, P.O. Box 11155-9161, Tehran, Iran*

²*ALBORZ Observatory, Sharif University of Technology, P.O. Box 11155-9161, Tehran, Iran*

³*Department of Physics, Payame Noor University, P.O. Box 19395-3697, Tehran, Iran*



(Received 23 July 2019; published 8 October 2019)

Using the CORSIKA code, in 21 energy states between 7 and 900 GeV, in each state, 2×10^4 extensive air showers were simulated separately with 88% protons and 12% alpha as primary particles. The zenith and azimuth angles of the primary particles were between 0° to 60° and 0° to 360° , respectively. These simulations are carried out at Tehran's level ($35^\circ 43' \text{N}$, $51^\circ 20' \text{E}$; 1200 m a.s.l = 897 g cm^{-2}) and with two models GHEISHA and UrQMD for hadronic interactions at low energy and the QGSJET-II model for high-energy interactions. Using the positive and negative muons produced from these air showers, the muon charge ratios are obtained at various angles and energies. An east-west anisotropy is also achieved for this ratio.

DOI: [10.1103/PhysRevD.100.083004](https://doi.org/10.1103/PhysRevD.100.083004)

I. INTRODUCTION

Muons are one of the flavors of leptons that have a rest energy of approximately 106 MeV and a mean lifetime of $2.2 \mu\text{s}$. The ratio of the number of positive to negative charge atmospheric muons reaching the Earth's surface is known as the muon charge ratio, R_μ . The charge ratio of the positive and negative muons, $R_\mu = n_+/n_-$, yields important information on the flux of atmospheric neutrinos and the hadron interactions. In the range of low-energy muons (approximately 1 GeV), the muon flux is an important source for the production of electron and muon neutrinos and antineutrinos, and the ratio of the number of positive to negative muons directly relates to the number of electron neutrinos to antineutrinos ($n_+/n_- = n_{\nu_e}/n_{\bar{\nu}_e}$). Since the interaction of positive and negative muons with the matter is not the same, finding the ratio of the positive to negative muons can be important for the response of neutrino detectors. Typically, positive and negative muons and relevant neutrinos and antineutrinos are produced from the decays in the atmosphere as

$$\begin{aligned}
 &A_{CR} + A_{\text{Air}} \rightarrow \pi^\pm + \pi^0 + K^\pm + \text{other hadrons}, \\
 &\left\{ \begin{array}{l} \pi^\pm \rightarrow \mu^\pm + \nu_\mu(\bar{\nu}_\mu); \quad \sim 100\%, \quad \tau_0 = 26 \text{ ns} \\ \downarrow \\ e^\pm + \nu_e(\bar{\nu}_e) + \bar{\nu}_\mu(\nu_\mu) \end{array} \right. , \\
 &\left\{ \begin{array}{l} K^\pm \rightarrow \mu^\pm + \nu_\mu(\bar{\nu}_\mu); \quad \sim 63.5\%, \quad \tau_0 = 12 \text{ ns} \\ \downarrow \\ e^\pm + \nu_e(\bar{\nu}_e) + \bar{\nu}_\mu(\nu_\mu), \end{array} \right.
 \end{aligned}$$

in which A_{CR} , A_{Air} , π^\pm , π^0 , and K^\pm represent a cosmic ray [such as a proton (P), alpha, and carbon (C) particles], an air nucleus, pions, and kaons, respectively. It is expected from these decays that the ratio of muon neutrinos to electron neutrinos, $(n_{\nu_\mu} + n_{\bar{\nu}_\mu})/(n_{\nu_e} + n_{\bar{\nu}_e})$, is equal to 2, but Super-Kamiokande experiments showed a smaller value for this ratio. This anomalous behavior was described based on the neutrino oscillations [1]. Muons at the ground surface are actually produced at high altitudes. Muons lose their energy by about $dE_\mu/dX = -2 \text{ MeV}/(\text{g cm}^{-2})$ due to ionization in the atmosphere. Regarding the relativistic effects, a muon with an energy of 1 GeV (i.e., with the Lorentz factor of $\gamma = 9.5$) has a lifetime of $\gamma\tau_0 \simeq 21 \mu\text{s}$ in the reference frame of an observer on the Earth's surface. Hence, it can reach Earth's surface from a height of more than $h = (\gamma^2 - 1)^{0.5} c\tau_0 \simeq 6.2 \text{ km}$, but due to the ionization loss, this height is reduced to about 3 km. As a result, the energy of the muons at Tehran's level is a convolution of the production spectrum, energy loss in the atmosphere, and decay.

In this paper, the positive and negative muons produced from primary particles, including protons (88%) and alpha (12%), with 21 energy states between 7 and 900 GeV, are separately identified for each energy. The muon charge ratio is obtained for each primary energy, and since the energy bins are not linearly selected but are rather quasilogarithmic, the mean value of muon charge ratio is calculated by weighting $E^{-1.7} \Delta(\log E)$. In these simulations, there are no restrictions on the energy of muons. Meanwhile, the east-west effect of the muon charge ratio has been studied in different energies of the primary generator particles.

*bahmanabadi@sina.sharif.edu

†fazlalizadeh.maedeh@gmail.com

II. GENERATED AIR SHOWERS WITH THE CORSIKA CODE

The CORSIKA (Cosmic Ray Simulations for Kascade; version 74000) program is used to simulate extensive air showers, initiated by proton, alpha, and different atomic nuclei as primary particles [2]. Various models of hadronic interaction are available in this program. The QGSJET (qgsjet01.f package) model [3] for hadronic interactions above $E_{\text{lab}} = 80$ GeV and the GHEISHA [4] and UrQMD [5] models for below $E_{\text{lab}} = 80$ GeV are used. These simulations were carried out at Tehran's level ($35^{\circ}43'N$, $51^{\circ}20'E$, 1200 m a.s.l = 897 g cm $^{-2}$), and the components of the geomagnetic field are $B_x = 27.97$ μT , $B_z = 39.45$ μT at this site and are taken from National Oceanic and Atmospheric Administration's National Centers for Environmental Information [6].

The geomagnetic field is assumed to be a constant value and independent of the angular direction of the muon. To describe this assumption, consider Fig. 1. The vertical height of atmosphere h_v is simply

$$h_v \simeq l \cos \theta + \frac{l^2}{2R_{\oplus}} \sin^2 \theta, \quad (l/R_{\oplus} \ll 1), \quad (1)$$

where l , θ , and R_{\oplus} are the length of a slant trajectory, zenith angle, and radius of the Earth, respectively. For $\theta \leq 60^{\circ}$, the second term in Eq. (1) can be disregarded. Suppose the latitude of the observation site is λ (Fig. 1). The variation in the latitude value of a muon from the start point to the end of the path $\Delta\lambda$ in terms of the zenith angle θ is given by the following trigonometric geometry:

$$\sin \Delta\lambda = \frac{l}{h_v + R_{\oplus}} \sin \theta. \quad (2)$$

The zenith angle distribution of muons can be represented by $\frac{dl}{d\theta} = 2\pi I_0 \sin \theta \cos^2 \theta$ [7]. The mean value of the zenith angle, between 0° and 60° , is $\bar{\theta} = \int_0^{\pi/3} \theta \cos^2 \theta \sin \theta d\theta / \int_0^{\pi/3} \cos^2 \theta \sin \theta d\theta = (9\sqrt{3} - \pi)/21$ rad $\simeq 34^{\circ}$.

With approximation $l \simeq h_v / \cos \theta$, for values $\theta = 34^{\circ}$, $h_v \simeq 20$ km, and $R_{\oplus} = 6400$ km, we obtain $\Delta\lambda \simeq 0.1^{\circ}$. With this value $\Delta\lambda$, the relative variation of the geomagnetic

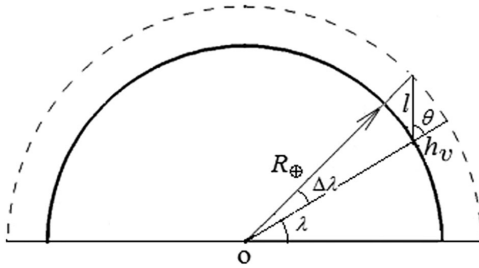


FIG. 1. A description of vertical height of atmosphere h_v , zenith angle θ , length of a slant trajectory l , the radius of the Earth R_{\oplus} , and other notations used in the text.

field components at the location of Tehran is calculated. With a dipole approximation for the geomagnetic field, i.e., $B_x = \frac{k}{r^3} \cos \lambda$ and $B_z = -\frac{2k}{r^3} \sin \lambda$, where for the Earth's dipole $k \simeq 8 \times 10^{15}$ Tm 3 , we obtain $|\frac{\Delta B_x}{B_x}| = 0.001$ and $|\frac{\Delta B_z}{B_z}| = 0.002$. The variation in the total magnetic field also becomes $\Delta B = [(B_x \Delta B_x)^2 + (B_z \Delta B_z)^2]^{0.5} / B \simeq 0.07$ μT . So, with a very small error, one can assume a uniform geomagnetic field.

Since the production of muons above 0.3 GeV (lower cutoff energy for muons in the CORSIKA code) at Tehran's level starts with energy 7 GeV for primary particles, to find the spectrum of muons and in turn to derive the muon charge ratio, the starting point for the primary particle energy was taken as 7 GeV. In this simulation, the energy of the primary particles was considered in 21 discrete states between 7 and 900 GeV. In each state, 2×10^4 air showers, including protons (88%) and alpha (12%) as primary particles and in all azimuthal angles and for zenith angles of up to 60° , were considered. The positive and negative muons produced from these simulations were used to derive the muon charge ratio.

III. SIMULATION RESULTS AND ANALYSIS METHOD

A. Direction and energy spectrum of muons

The coordinate axes in the CORSIKA program are defined as in Fig. 2. The positive direction of the x and y axes are towards the north and the west, respectively. The zenith θ and azimuth ϕ angles are indicated in Fig. 2. Using the momentum components of muons available in the simulation output data, zenith and azimuth angles are calculated as follows:

$$\cos \theta = \frac{p_z}{\sqrt{p_x^2 + p_y^2 + p_z^2}}, \quad \sin \phi = \frac{p_y}{\sqrt{p_x^2 + p_y^2}}. \quad (3)$$

The energy of each muon is also obtained using its momentum, $E_{\mu} = (p^2 c^2 + m_0^2 c^4)^{0.5}$. The energy spectra of muons produced from proton (88%) and alpha (12%) as

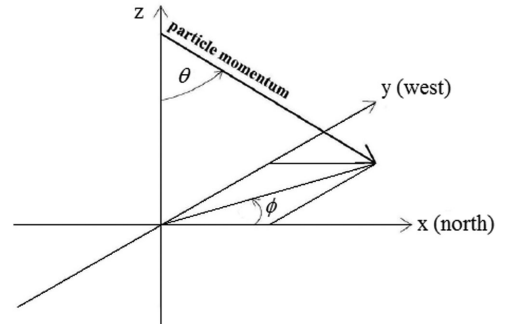


FIG. 2. Coordinate system in the CORSIKA program.

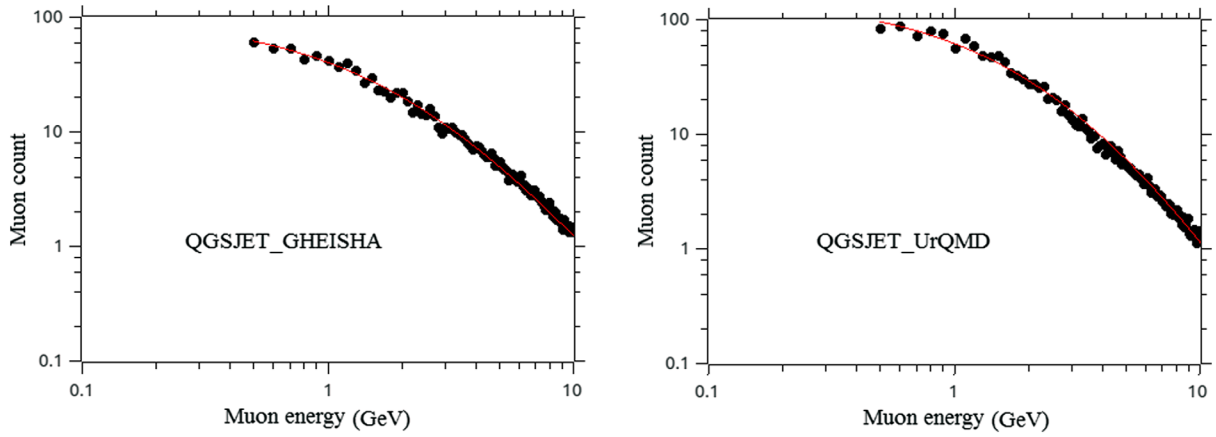


FIG. 3. Energy spectra of the muons at Tehran's level with models QGSJET-GHEISHA (left) and QGSJET-UrQMD (right). Solid curves show the fit of the data with Eq. (4).

primary particles in 21 discrete energies between 7 and 900 GeV, and with a differential flux given by $dN/dE \propto E^{-2.7}$ and in zenith angles of 0° to 60° , with two sets of models QGSJET- GHEISHA and QGSJET-UrQMD are shown in Fig. 3. The distributions are fitted with a function as [8]

$$\frac{dN(E_\mu)}{dE_\mu} = A(E_0 + E_\mu)^{-\gamma}, \quad (4)$$

where the values of the fit parameters for Tehran's level are $A = (1.1 \pm 0.4, 9.7 \pm 7.1) \times 10^3 (\text{GeV})^{\gamma-1}$, $E_0 = (2.4 \pm 0.2, 3.2 \pm 0.4) \text{ GeV}$, and $\gamma = (2.7 \pm 0.2, 3.5 \pm 0.3)$, where the first values of each of the sets of parentheses belong to the QGSJET- GHEISHA model and the second values of which belong to the QGSJET-UrQMD model. The slope of these spectra at energy less than 1 GeV is almost flat and gradually increases.

TABLE I. Number of positive and negative muons produced in various primary particle energies and the corresponding muon charge ratio values with two sets of models QGSJET- GHEISHA (Q-G) and QGSJET-UrQMD (Q-U) without any restriction on muon energy.

Primary particle energy E (GeV)	(Q-G)			(Q-U)		
	n_+	n_-	R_μ	n_+	n_-	R_μ
7	26	16	1.63 ± 0.52	59	52	1.13 ± 0.22
8	50	35	1.43 ± 0.31	135	93	1.45 ± 0.20
9	111	83	1.34 ± 0.19	170	162	1.05 ± 0.12
10	167	126	1.33 ± 0.16	306	242	1.26 ± 0.11
20	1563	1271	1.23 ± 0.05	1879	1580	1.19 ± 0.04
30	3587	2982	1.20 ± 0.03	4118	3293	1.25 ± 0.03
40	6266	5125	1.22 ± 0.02	6670	5599	1.19 ± 0.02
50	9518	7862	1.21 ± 0.02	9234	7946	1.16 ± 0.02
60	12 345	10 456	1.18 ± 0.02	11 684	10 167	1.15 ± 0.02
70	15 358	13 044	1.18 ± 0.01	14 388	12 728	1.13 ± 0.01
80	18 338	15 480	1.18 ± 0.01	16 969	14 880	1.14 ± 0.01
90	21 025	18 187	1.16 ± 0.01	21 262	18 603	1.14 ± 0.01
100	23 718	20 620	1.15 ± 0.01	23 815	20 710	1.15 ± 0.01
200	50 677	45 357	1.12 ± 0.01	49 796	45 290	1.10 ± 0.01
300	74 107	68 606	1.08 ± 0.01	72 614	67 731	1.07 ± 0.01
400	96 557	90 082	1.07 ± 0.00	95 350	89 489	1.07 ± 0.00
500	118 160	110 704	1.07 ± 0.00	115 584	110 259	1.05 ± 0.00
600	136 505	129 501	1.05 ± 0.00	134 724	128 783	1.05 ± 0.00
700	155 943	147 778	1.06 ± 0.00	153 790	147 680	1.04 ± 0.00
800	174 822	166 018	1.05 ± 0.00	170 788	165 302	1.03 ± 0.00
900	193 839	184 719	1.05 ± 0.00	189 926	183 432	1.04 ± 0.00
Mean value	1634	1389	1.18 ± 0.04	1758	1517	1.16 ± 0.04

B. Muon charge ratio dependence on the primary particle energy

In 21 different energies for proton and alpha particles, the number of positive and negative muons produced by them was obtained. The number of positive and negative muons produced in various primary particle energies and with two sets of models QGSJET- GHEISHA and QGSJET-UrQMD are presented in Table I. The calculated values for the muon charge ratio, $R_\mu = n_+/n_-$, are also given in this table. The standard deviation is obtained as $\sigma = (n_+^2 n_- + n_-^2 n_+)^{0.5}/n_-^2$. The differential energy spectrum of the primary particles is $dN/dE \propto E^{-2.7}$, but since in the simulations the energy bins are not linearly selected but are rather quasilogarithmic, the mean value of \bar{n}_\pm is calculated as follows:

$$\bar{n}_\pm = \frac{\sum_{i=1}^{21} n_{\pm i} E_i^{-1.7} \Delta(\log E_i)}{\sum_{i=1}^{21} E_i^{-1.7} \Delta(\log E_i)}. \quad (5)$$

In this way, the mean values of (n_+, n_-) , without any restriction on muons energy, for two sets of models QGSJET-GHEISHA and QGSJET-UrQMD, are about (1634, 1389) and (1758, 1517), respectively. Thus, the values of the muon charge ratio for these two models are 1.18 ± 0.04 and 1.16 ± 0.04 , respectively.

It can be seen that the predictions of the QGSJET-GHEISHA model are more compatible with experimental result [7]. An overall comparison in Table I shows that below energy 50 GeV for primary particles UrQMD produces positive and negative muons more than GHEISHA and reverses at higher energies. In almost all primary energies, the muon charge ratio in GHEISHA is higher than in UrQMD. This indicates that GHEISHA is more sensitive to the production of positive muons. The mean values of the muon charge ratio for the two sets of models QGSJET-GHEISHA and QGSJET-UrQMD are 1.18 ± 0.04 and 1.16 ± 0.04 , respectively, which shows a relative difference about 2% between the GHEISHA and UrQMD models.

C. Azimuthal anisotropy

Using Eq. (3), one can obtain the azimuth angle ϕ of each muon by having its momentum components and thereby identify their east-west orientation. Table II displays the muon charge ratios from east R_E and west R_W half-space in different energies of primary particles obtained with the CORSIKA code and with the two sets of models QGSJET-GHEISHA and QGSJET-UrQMD for hadronic interactions. The mean muon charge ratio in the east and west direction, over the whole energies with a weight $E^{-1.7} \Delta(\log E)$, can be calculated. These values are presented in Table II for the two sets of models. By introducing the azimuthal anisotropy as $A_{EW} = 2(R_W - R_E)/(R_W + R_E)$, for the mean values of the muon charge ratio, the anisotropy values are 0.15 ± 1.30

TABLE II. The muon charge ratio from east and west half-space in different energies of primary particles obtained with CORSIKA and with the two sets of models QGSJET-GHEISHA (Q-G) and QGSJET-UrQMD (Q-U).

Primary particle energy E (GeV)	(Q-G)		(Q-U)	
	R_E	R_W	R_E	R_W
7	2.00 ± 0.93	1.33 ± 0.59	1.08 ± 0.29	1.19 ± 0.32
8	1.09 ± 0.32	2.00 ± 0.68	1.18 ± 0.22	1.79 ± 0.34
9	1.02 ± 0.21	1.75 ± 0.37	1.13 ± 0.18	0.98 ± 0.15
10	1.27 ± 0.22	1.38 ± 0.23	1.07 ± 0.13	1.48 ± 0.18
20	1.12 ± 0.06	1.35 ± 0.07	1.07 ± 0.05	1.31 ± 0.06
30	1.12 ± 0.04	1.29 ± 0.05	1.17 ± 0.04	1.33 ± 0.04
40	1.12 ± 0.03	1.33 ± 0.04	1.07 ± 0.03	1.33 ± 0.03
50	1.10 ± 0.02	1.33 ± 0.03	1.07 ± 0.02	1.27 ± 0.03
60	1.10 ± 0.02	1.27 ± 0.02	1.08 ± 0.02	1.22 ± 0.02
70	1.11 ± 0.02	1.26 ± 0.02	1.04 ± 0.02	1.22 ± 0.02
80	1.11 ± 0.02	1.26 ± 0.02	1.07 ± 0.02	1.22 ± 0.02
90	1.10 ± 0.02	1.22 ± 0.02	1.08 ± 0.02	1.21 ± 0.02
100	1.09 ± 0.01	1.22 ± 0.02	1.07 ± 0.01	1.24 ± 0.02
200	1.05 ± 0.01	1.18 ± 0.01	1.04 ± 0.01	1.16 ± 0.01
300	1.03 ± 0.01	1.13 ± 0.01	1.01 ± 0.01	1.14 ± 0.01
400	1.03 ± 0.01	1.12 ± 0.01	1.01 ± 0.01	1.12 ± 0.01
500	1.02 ± 0.01	1.12 ± 0.01	1.00 ± 0.01	1.10 ± 0.01
600	1.00 ± 0.01	1.11 ± 0.01	0.99 ± 0.01	1.10 ± 0.01
700	1.01 ± 0.01	1.11 ± 0.01	1.00 ± 0.01	1.09 ± 0.01
800	1.01 ± 0.00	1.10 ± 0.01	0.98 ± 0.00	1.08 ± 0.01
900	1.00 ± 0.00	1.10 ± 0.01	0.99 ± 0.00	1.08 ± 0.01
Mean value	1.09 ± 0.06	1.27 ± 0.07	1.07 ± 0.05	1.25 ± 0.06

and 0.15 ± 1.31 for the two sets of models QGSJET-GHEISHA and QGSJET-UrQMD, respectively. The standard deviation is obtained as $\sigma = 4(R_E^2 R_W + R_W^2 R_E)^{0.5}/(R_W + R_E)^2$. These results show a pronounced east-west effect.

The east-west effect, the details of which have been investigated in numerous studies, for example, in Refs. [9–12], is actually the interaction of the geomagnetic field with secondary charged particles, especially with muons [13–15]. Figure 4 shows a schematic description

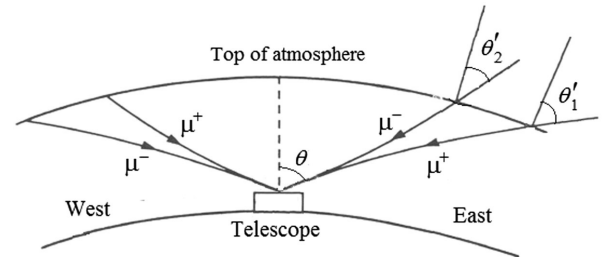


FIG. 4. Schematic description of the east-west effect of atmospheric muons.

of this effect on muons. When positive and negative muons arrive at the ground level with a certain zenith angle θ , they have actually been produced by different air showers and due to different charge signs find different bending in geomagnetic field. The bending of muons depends on their movement in the east or west direction. In fact, low-energy muons are deflected in the geomagnetic field at large zenith angles. The deflection angle is approximately

$$\psi = \frac{l}{r}. \quad (6)$$

Here, l and r are the path length and curvature radius of a muon, respectively. For a muon with momentum p and total energy E , the radius of curvature in the magnetic field B is $r = \frac{pc}{ecB} \approx \frac{E}{ecB}$. For a magnetic field $B \approx 0.5 \times 10^{-4}$ T, the curvature radius in meters is $r \approx 0.67 \times 10^5 (\frac{E}{1 \text{ GeV}})$. So, for a muon with energy 1 GeV and zenith angle $\theta = 34^\circ$ and with a vertical height of atmosphere $h_v = 20$ km, the deflection angle is about $\psi \approx 0.36 \text{ rad} \approx 21^\circ$. In the east direction, the path length of a positive muon is longer than a negative muon. So, Positive and negative muons reaching the telescope with the identical zenith angle, θ , in fact at the top of the atmosphere are produced at different zenith angles $\theta'_1 = \theta + \psi$ and $\theta'_2 = \theta - \psi$ respectively, as shown in Fig. 4. This event on the west side is just the opposite, and the length of the positive muon path is shorter (Fig. 4). So, on the one hand, the number of atmospheric positive muons is more than the negative muons, and on the other hand, at a certain angle, the path length of positive muons is less than the negative muons in the west direction relative to the east. Therefore, these features indicate how the different bending of the trajectories of positive and negative muons in the geomagnetic field causes a west-east effect.

IV. CONCLUSION

The charge ratio of the atmospheric muons, produced by extensive air showers, is a quantity sensitive to the

hadron interaction models and the geomagnetic field. In this paper, we presented the effect of GHEISHA and UrQMD models on the production of positive and negative muons. The results obtained from the CORSIKA simulation are as follows:

- (1) The obtained data show that the number of positive and negative muons increases with increasing initial particle energy. If we consider the total number of positive and negative muons produced in terms of a function of the primary particle energy, it can be seen that before 50 GeV the UrQMD produces more muons than GHEISHA and then reverses. In almost all primary energies, the muon charge ratio in GHEISHA is higher than in UrQMD. This indicates that GHEISHA is more sensitive to the production of positive particles. The mean values of the muon charge ratio for the two sets of models QGSJET-GHEISHA and QGSJET-UrQMD are 1.18 ± 0.04 and 1.16 ± 0.04 , respectively, which shows a relative difference about 2% between the GHEISHA and UrQMD models.
- (2) The mean values of the muon charge ratio in the direction of the half-space of the east and west with the model QGSJET-GHEISHA are 1.09 ± 0.06 and 1.27 ± 0.07 , respectively, and with the model QGSJET-UrQMD are 1.07 ± 0.05 and 1.25 ± 0.06 , respectively. This anisotropy of the east-west is due to the geomagnetic field effect on the charged muons.
- (3) The results of the model QGSJET-GHEISHA are more consistent with the experiments than the model QGSJET-UrQMD.

ACKNOWLEDGMENTS

This research was supported by a grant from the Office of Vice President for Science, Research and Rechnology of Sharif University of Technology. The authors thank the anonymous referee for his valuable comments.

-
- | | |
|--|---|
| <p>[1] T. K. Gaisser and T. Stanev, <i>Phys. Rev. D</i> 38, 85 (1988).
 [2] D. Heck <i>et al.</i>, Forschungszentrum Karlsruhe Report No. FZKA6019, 1998.
 [3] N. N. Kalmykov and S. S. Ostapchenko, <i>Yad. Fiz.</i> 56, 105 (1993) [<i>Phys. At. Nucl.</i> 56, 346 (1993)]; N. N. Kalmykov, S. S. Ostapchenko, and A. I. Pavlov, <i>Izv. RAN Ser. Fiz.</i> 58, 21 (1994); <i>Bull. Russ. Acad. Science (Physics)</i> 58, 1966 (1994); <i>Nucl. Phys. B, Proc. Suppl.</i> 52, 17 (1997).
 [4] H. Fesefeldt (GHEISHA Collaboration), RWTH Aachen Report No. PITHA-85/02, 1985 (unpublished).</p> | <p>[5] S. A. Bass <i>et al.</i>, <i>Prog. Part. Nucl. Phys.</i> 41, 255 (1998).
 [6] https://www.ngdc.noaa.gov/geomag-web/.
 [7] S. Abdollahi, M. bahmanabadi, and D. Purmohammad, <i>J. Phys. G</i> 40, 025202 (2013).
 [8] M. bahmanabadi and L. Rafezi, <i>Phys. Rev. D</i> 98, 103003 (2018).
 [9] J. Wentz, A. F Badaea, A. Bercuci, H. Bozdog, I. M. Brancus, H.-J. Mathes, M. Petcu, H. Rebel, and B. Vulpescu, <i>J. Phys. G</i> 27, 1699 (2001); <i>Phys. Rev. D</i> 67, 073020 (2003).</p> |
|--|---|

-
- [10] P. Lipari, T. Stanev, and T. K. Gaisser, *Phys. Rev. D* **58**, 073003 (1998).
- [11] C. Stormer, *Astrophysics* **1**, 237 (1930).
- [12] J. Wentz, A. Bercuci, and B. Vulpescu, *Proc. 27th ICRC, Hamburg* (Copernicus Gesellschaft, Hamburg, Germany, 2001), Vol. 3, p. 1167.
- [13] O. C. Allkofer, W. D. Dau, H. Jokisch, G. Klemke, R. C. Uhr, G. Bella, and Y. Oren, *J. Geophys. Res.* **90**, 3537 (1985).
- [14] T. Futagami *et al.* (Super-Kamiokande Collaboration), *Phys. Rev. Lett.* **82**, 5194 (1999).
- [15] P. Lipari, *Astropart. Phys.* **14**, 171 (2000).